Title	Self-attraction and loading effects on ocean mass redistribution at monthly and longer time scales.
Author(s)	Vinogradova, N. T.; Ponte, R. M.; Tamisiea, M. E.; Quinn, K. J.; Hill, Emma M.; Davis, J. L.
Citation	Vinogradova, N. T., Ponte, R. M., Tamisiea, M. E., Quinn, K. J., Hill, E. M., & Davis, J. L. (2011). Self-attraction and loading effects on ocean mass redistribution at monthly and longer time scales. Journal of Geophysical Research, 116.
Date	2011
URL	http://hdl.handle.net/10220/8802
Rights	© 2011 American Geophysical Union. This paper was published in Journal of Geophysical Research and is made available as an electronic reprint (preprint) with permission of American Geophysical Union. The paper can be found at: [DOI: http://dx.doi.org/10.1029/2011JC007037]. One print or electronic copy may be made for personal use only. Systematic or multiple reproduction, distribution to multiple locations via electronic or other means, duplication of any material in this paper for a fee or for commercial purposes, or modification of the content of the paper is prohibited and is subject to penalties under law.

Self-attraction and loading effects on ocean mass redistribution at monthly and longer time scales

N. T. Vinogradova,[1] R. M. Ponte,[1] M. E. Tamisiea,[2] K. J. Quinn,[1] E. M. Hill,[3,4] and J. L. Davis[3,5]

Received 4 February 2011; revised 9 May 2011; accepted 27 May 2011; published 31 August 2011.

[1] Self-attraction and loading (SAL) effects caused by changes in mass loads associated with land hydrology, atmospheric pressure, and ocean dynamics produce time-varying, nonuniform spatial patterns in ocean bottom pressure (OBP). Such mass redistribution produced by SAL effects is shown to be an important component of OBP variability on scales from months to years and to provide for a better description of the OBP annual cycle observed by GRACE (Gravity Recovery and Climate Experiment). The SAL-induced ocean mass variations have magnitudes comparable to the dynamic OBP signals at subannual, annual, and interannual time scales in many ocean regions and should not be ignored in studies of ocean mass. Annual variations account for the most variability in SAL-related mass signals and can be induced by all the loads considered, with hydrology having the largest contribution. At subannual and interannual time scales, impact of hydrology is minimal and variations are mostly related to load changes from ocean dynamics and from changes in atmospheric circulation, depending on ocean region. The results demonstrate that the large-scale SAL effects are not negligible in the analysis of GRACE-derived global observations of OBP. The estimated SAL effects can explain on average 0.2 cm^2 (16%) of the variance in the GRACE annual cycle (expressed in terms of equivalent water height), exceeding 1 cm^2 in both open ocean and coastal regions with strong annual SAL signals.

Citation: Vinogradova, N. T., R. M. Ponte, M. E. Tamisiea, K. J. Quinn, E. M. Hill, and J. L. Davis (2011), Self-attraction and loading effects on ocean mass redistribution at monthly and longer time scales, *J. Geophys. Res.*, *116*, C08041, doi:10.1029/2011JC007037.

1. Introduction

[2] Any change in mass loads over the globe, be it related to variability in the atmosphere, land or oceans, represents changes in the gravity field associated not just with self-gravitation but also with crustal deformation processes. Such gravity field perturbations act essentially as a body force on the oceans and the resulting adjustments in the mass (or sea level) fields are commonly referred to as self-attraction and loading (SAL) effects after *Gordeev et al.* [1977]. The physics of SAL have been of interest for several decades particularly because of the associated spatially varying long term trends in sea level that can result from the melting of land ice [e.g., *Farrell and Clark*, 1976; *Clark and Primus*, 1987; *Nakiboglu and Lambeck*, 1991; *Conrad and Hager*, 1997; *Mitrovica et al.*, 2001; *Riva et al.*, 2010]. Effects of SAL have also been shown to be an essential part of barotropic ocean dynamics on rapid time scales, including ocean free oscillations [*Muller*, 2007], tides [*Hendershott*, 1972; *Gordeev et al.*, 1977; *Ray*, 1998], and atmospherically forced motions [*Stepanov and Hughes*, 2004]. The impact of SAL on the full spectrum of oceanic variability, including monthly to interannual time scales, has not been examined in any detail, however.

[3] Works by *Tamisiea et al.* [2010] and *Vinogradova et al.* [2010] have recently highlighted the importance of SAL effects to the understanding of the annual cycle in relative sea level and in bottom pressure (ξ). Inclusion of SAL physics cause spatial variations in sea level and ξ annual amplitudes that can exceed 1 cm. While past studies have mostly focused on the role of SAL in affecting sea level patterns [e.g., *Clarke et al.*, 2005; *Mitrovica et al.*, 2001; *Wouters et al.*, 2011], the findings of *Tamisiea et al.* [2010] and *Vinogradova et al.* [2010] are particularly relevant for ξ studies. Because changes in sea level are mostly related to those in steric height, which imply no change in mass or ξ, variability in sea level tends to be substantially larger than

[1] Atmospheric and Environmental Research, Inc., Lexington, Massachusetts, USA.
[2] National Oceanography Centre, Liverpool, UK.
[3] Harvard-Smithsonian Center for Astrophysics, Cambridge, Massachusetts, USA.
[4] Now at Earth Observatory of Singapore, Nanyang Technological University, Singapore, Singapore.
[5] Now at Lamont-Doherty Earth Observatory, Columbia University, Palisades, New York, USA.

0148-0227/11/2011JC007037

that in ξ over most of the oceans. Dynamic variability in ξ, which partly reflects small imbalances in mass fluxes associated with Ekman and geostrophic flows or surface freshwater input [*Gill and Niiler*, 1973; *Ponte*, 1999], is relatively small (~1–2 cm during a year) over most of the ocean [*Vinogradova et al.*, 2007; *Ponte*, 1999]. For comparison, typical amplitude of seasonal fluctuations of sea level is around 4–6 cm [*Vinogradov et al.*, 2008]. Thus, as described by *Vinogradova et al.* [2010], magnitudes of SAL effects are comparable to expected dynamic ξ signals, making their treatment very important when interpreting ξ measurements.

[4] The implications of SAL for ξ analyses gain considerable importance in light of mounting ξ records derived from satellite geodesy missions such as GRACE (Gravity Recovery and Climate Experiment). Previous studies have shown that ocean mass variability derived from GRACE is generally in qualitative agreement with other model-based ξ estimates [*Ponte et al.*, 2007; *Chambers*, 2006; *Quinn and Ponte*, 2008], but in many ocean regions GRACE tends to display larger variability. Given that most ocean models do not include SAL physics in their formulations, a pertinent question in light of the *Vinogradova et al.* [2010] results is whether those missing physics could account for some of the discrepancies between model and GRACE estimates of ξ.

[5] In the present paper, we extend the analysis of *Vinogradova et al.* [2010] and examine for the first time the magnitude and importance of SAL effects at frequencies other than annual, in comparison to other natural variability in ξ fields on a range of time scales, and in the novel context of the global GRACE observations. Depending on ocean region, annual variations in ξ might not be necessarily the largest, with fluctuations at other (typically higher) frequencies dominating the ξ spectra. Variations in ξ at interannual scales, even if typically smaller, serve as important indicators of climate change resulting, for example, from variable melting rates of glaciers and ice sheets. The analysis of SAL effects on different time scales will include loads from land hydrology, atmosphere and ocean dynamics and help build a comprehensive description of the nature and causes of the SAL-induced changes over the ocean. The comparisons with GRACE allow for the evaluation of SAL effects over the global ocean, as opposed to just at a few in situ locations as with *Vinogradova et al.* [2010], and are intended to clarify the nature of ξ variability observed by GRACE and the differences with model-based ξ estimates, in terms of possible data and model shortcomings.

2. Methods, Data, and Models

[6] To assess the importance of SAL effects on ξ, we use ξ_{SAL} monthly fields derived as described in detail by *Tamisiea et al.* [2010]. Their approach involves the solution of the so-called "sea level equation" in an iterative procedure to estimate the spatial distribution of crustal displacement and gravitational changes resulting from the various mass loads, under the assumption that the ocean response to these loads is static, i.e. the applied loading is balanced by the resulting ξ gradients.

[7] Three different loads are considered: (1) the global hydrological cycle, particularly its land component; (2) dynamic ξ variations associated with redistribution of mass in the ocean driven by atmospheric forcing or intrinsic ocean processes; and (3) atmospheric mass variations as represented by changes in surface pressure over land (over the ocean, only changes in the spatial mean atmospheric pressure matter, as the ocean tends to respond isostatically to any imposed spatial gradients in surface pressure [e.g., *Ponte*, 1999]). The loads are based on the hydrological fields from GLDAS (Global Land Data Assimilation System) [*Rodell et al.*, 2004], dynamic ocean pressure from the data-constrained ECCO solutions described by *Wunsch et al.* [2009], and atmospheric pressure from NCEP-NCAR reanalysis [*Kalnay et al.*, 1996]. It should be noted that these input fields are monthly averages. Thus, subannual variations have explicitly excluded submonthly changes. In addition, the input from hydrological and cyrospheric loads in Greenland and Antarctica include only the annual components [see *Tamisiea et al.*, 2010], thus the relative importance of the hydrology-driven ξ_{SAL} variations may be underrepresented, particularly in these regions.

[8] Following *Vinogradova et al.* [2010], the resulting perturbations in ξ under individual loads are referred to as ξ_{SAL_H}, ξ_{SAL_D}, and ξ_{SAL_A}, respectively, and expressed in units of equivalent centimeters of water, i.e., units of normalized bottom pressure $\xi/g\rho_0$, where constants g and ρ_0 are the acceleration of gravity and mean seawater density. The hydrological and atmospheric fields are those used by *Tamisiea et al.* [2010]. For dynamic ξ variations, we use monthly averaged fields from a recent ECCO solution (version 3, iteration 73 [see *Wunsch et al.*, 2009]), which includes effects of sea ice through dynamic/thermodynamical sea ice model [*Losch et al.*, 2010] and extends until the end of 2008. The ECCO solution is based on a least squares fit of the MIT general circulation model to a variety of observations to produce an optimized estimate of the ocean state. (We note that results based on ECCO unconstrained solutions, with no optimization involved, were also considered but did not differ significantly from those discussed here). The present configuration uses the Boussinesq approximation and an implicit free surface.

[9] In our analysis, we remove the time-dependent global mean from values of ξ_{SAL} and deal mostly with deviations

$$\Delta\xi_{SAL} = \xi_{SAL} - \overline{\xi}_{SAL} \tag{1}$$

The spatial mean $\overline{\xi}_{SAL}$ represents the net freshwater transfers into the ocean from land and atmosphere as well as the effects of changes in mean atmospheric mass over the oceans. While $\overline{\xi}_{SAL}$ is a focus of most ocean mass balance studies and contains relatively large variability (for example, the annual mean mass change is about 1 cm in amplitude), the essence of SAL physics is revealed in the deviations $\Delta\xi_{SAL}$, as described by *Vinogradova et al.* [2010] and others. Moreover, spatially constant temporal variations represented by $\overline{\xi}_{SAL}$ have no associated pressure gradients and are not important for the interpretation of ξ variability in terms of ocean currents and dynamics. The spatially varying $\Delta\xi_{SAL}$ signals are thus the main subject of the present study.

[10] To analyze relative importance of the $\Delta\xi_{SAL}$ effects, we compare these terms with the expected variations in ξ as estimated in the ECCO solution (ξ_d) and as observed by the satellite gravity mission GRACE. For the GRACE data (d) we use monthly gridded maps of ξ [*Quinn and Ponte*, 2008] for 2002–2008, from global spherical harmonic solutions

produced by the University of Texas Center for Space Research (CSR), Release 4. The spherical harmonic gravity coefficients are used up to degree and order 60 and smoothed with a 750 km width Gaussian filter. Additionally, the GRACE fields are "destriped" to remove correlated errors that produce characteristic north-south stripes [*Chambers*, 2006; *Swenson and Wahr*, 2006], the C_{20} values are replaced by satellite laser ranging estimates, and seasonal degree 1 terms from *Eanes* [2000] are added. We also add back the GAD ocean and atmosphere background model to obtain the total mass variability over the ocean. Full details of these GRACE data processing steps are given by *Quinn and Ponte* [2008]. To be consistent with the GRACE data, ξ_d and $\Delta\xi_{SAL}$ grids were also smoothed in the spherical harmonic domain with 750 km width Gaussian filter. Finally, the spatial average over the ocean is removed from ξ_d and d grids.

[11] It is worth noting that, while smoothing reduces systematic errors in the GRACE data, it also reduces its spatial resolution. As a result of the low spatial resolution, some of the near-field GRACE data could be contaminated by the land signals, where the mass changes are much larger than the ocean effects. Previous studies [e.g., *Wahr et al.*, 1998; *Chambers et al.*, 2007; *Chambers*, 2009; *Quinn and Ponte*, 2010] suggest masking out the continental regions to reduce land signal leakage over the ocean. Although the applied techniques are shown to reduce the bias in the ocean mass estimates, it is unlikely that all the leakage is being removed. In this study we explore the effect of different land masks on leakage and SAL effects by extending ocean boundaries from the continents by 200, 300, and 400 km in order to exclude coastal regions with the highest land signal contamination.

[12] The impact of $\Delta\xi_{SAL}$ effects is estimated in terms of explained GRACE variance, i.e.,

$$\alpha_0 = \frac{\sigma^2(d) - \sigma^2(d - \xi_d)}{\sigma^2(d)} \times 100\% \tag{2}$$

$$\alpha_1 = \frac{\sigma^2(d) - \sigma^2(d - (\xi_d + \xi_{SAL}))}{\sigma^2(d)} \times 100\% \tag{3}$$

$$\Delta\alpha = \alpha_1 - \alpha_0 \tag{4}$$

where α_0 and α_1 are percentages of the observed variance explained by ξ_d without and with consideration of SAL effects, respectively. The value of $\Delta\alpha$ is a quantitative measure of the extra variance explained by adding $\Delta\xi_{SAL}$ effects to the ECCO ξ_d fields ($\Delta\alpha > 0$ implies that inclusion of SAL effects improves the agreement with the observations).

[13] Our analysis is focused on the period 2002–2008, corresponding to the years of overlap in the GRACE and ECCO solution. We examine the SAL effects as a function of time scale and load. The time scales of interest are interannual, annual, and subannual. The annual cycle in $\Delta\xi_{SAL}$ corresponds to the mean annual cycle that is estimated from climatology computed over the 7 year period of analysis. Interannual and subannual anomalies are obtained by removing the annual cycle and linear trend from the original series and then applying a low/high-pass filter to remove anomalies at periods shorter/longer than 12 months. Throughout the paper, variability is defined in terms of standard deviations of $\Delta\xi_{SAL}$ time series at the analyzed frequency bands.

3. Spatial and Temporal Variations of SAL Effects

[14] Figure 1a shows the standard deviation of ξ_{SAL} representing variability at all time scales, including any linear trends, present in the 7 year period of study. Typical values of ~1 cm result from all effects (land hydrology, atmosphere, and ocean dynamics) and include variability in the mean atmospheric mass over the ocean, as well as changes in the mean oceanic mass associated with net water mass transfers from land and atmosphere. The effects of SAL physics lead to spatially nonuniform mass redistribution within the ocean, which is best isolated by removing the time-varying spatial mean and considering the deviations $\Delta\xi_{SAL}$. Variability in $\Delta\xi_{SAL}$ (Figure 1b) is understandably smaller, with typical standard deviations of a few millimeters over the deep ocean, approaching 1 cm in several coastal areas.

[15] To assess the importance of $\Delta\xi_{SAL}$ signals in analyses of ξ, we compare the variability in $\Delta\xi_{SAL}$ with that of the dynamic ocean bottom pressure ξ_d as estimated from the ECCO solution during the same time period. Variability in ξ_d, shown in Figure 1c, is typically <2 cm over most of the deep ocean, with larger values in several coastal regions, as described in detail in previous studies [e.g., *Vinogradova et al.*, 2007; *Ponte*, 1999]. The ratio of variability in $\Delta\xi_{SAL}$ to that in ξ_d (Figure 1d) is significant in many ocean regions and ranges from about 0.1–0.4 in the open ocean (largest ratios in tropical latitudes) to >0.5 in many coastal regions. *Vinogradova et al.* [2010] showed that $\Delta\xi_{SAL}$ and ξ_d have comparable amplitudes at annual frequencies in many coastal regions. Some of the largest ratios in Figure 1d are thus dominated by the annual cycle. A similar comparison between $\Delta\xi_{SAL}$ and ξ_d is done in Figures 1e and 1f after removing an annual cycle and linear trend from both fields. In this case, coastal ratios are indeed smaller. However, ratios over the deep ocean are similar to those in Figure 1d, indicating that the magnitude of SAL signals are also not negligible at frequencies other than annual, and that ignoring $\Delta\xi_{SAL}$ can potentially lead to problems in the interpretation or simulation of ξ variability at a variety of time scales.

[16] To understand in better detail the spatial patterns seen in Figure 1, we examine the nature and magnitude of $\Delta\xi_{SAL}$ variability as a function of each load (hydrology, atmosphere, ocean) and time scale. As seen from Figure 2e (cf. Figures 2a and 2i), variations at annual time scales account for the most variability in $\Delta\xi_{SAL}$ in many ocean areas, including coastal oceans and some open ocean regions (e.g., Indian Ocean and the South Pacific). Annual variations can be induced by all loads considered here, depending on ocean region. For example, ξ_{SAL_H} is the dominant cause of annual variation along the continents in the northern hemisphere and the areas around the Amazon river basin (Figure 2f). Ocean dynamics ξ_{SAL_D} is a primary cause of the annual

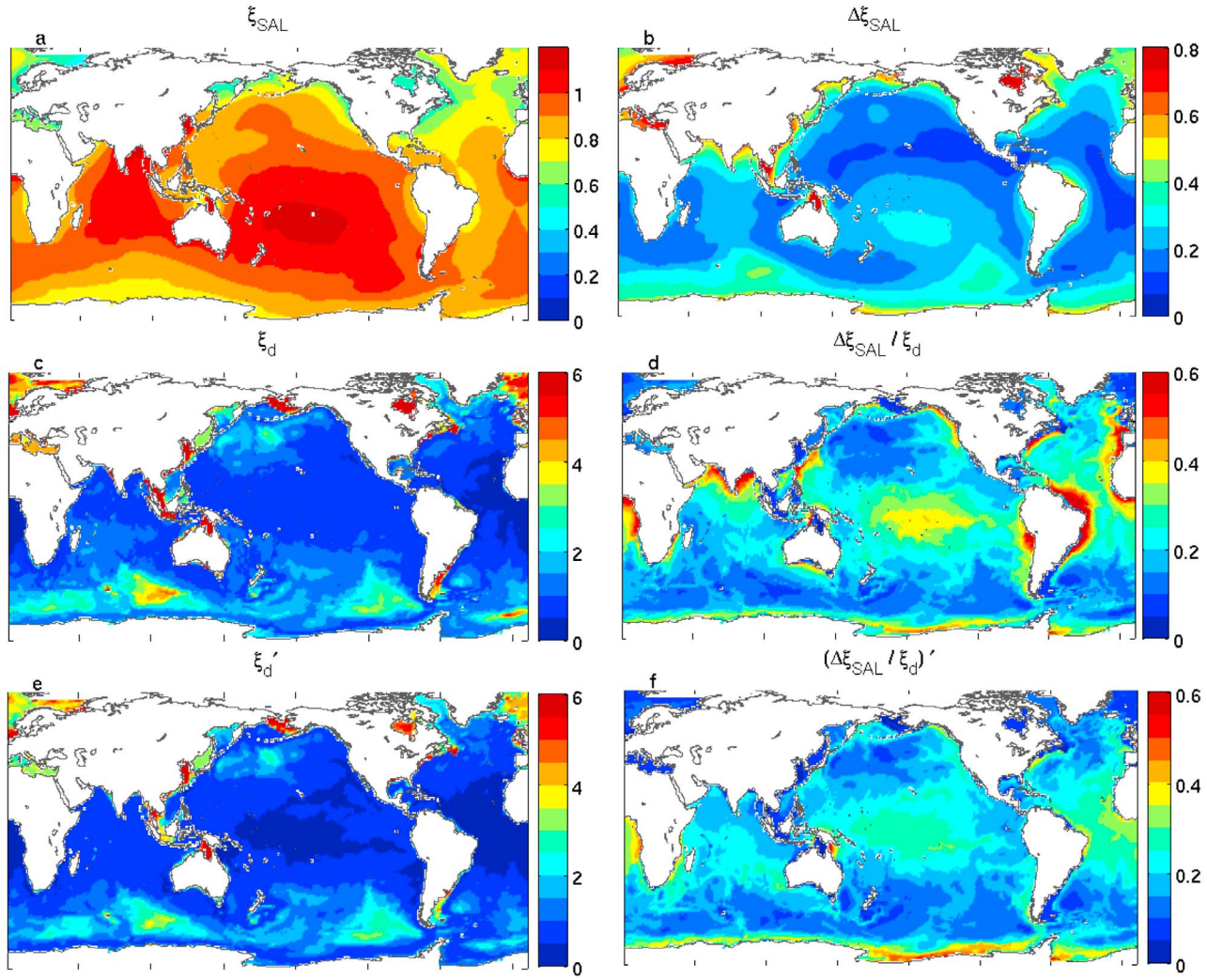

Figure 1. Variability (standard deviation) of (a) SAL-induced ξ fluctuations including spatial mean term ($\Delta\xi_{SAL} + \bar{\xi}_{SAL}$), (b) SAL-induced ξ signal without spatial mean ($\Delta\xi_{SAL}$), (c and e) dynamic bottom pressure variations (with spatial mean removed) estimated from ECCO solution (ξ_d), and (d and f) ratio $\Delta\xi_{SAL}/\xi_d$. Variability is computed based on a 7 year period from 2002 to 2008: Figures 1c and 1d contain all time scales, including trends, and Figures 1e and 1f show variability with trends and annual cycle removed. Units are equivalent cm of water thickness.

variations in some parts of the Southern Ocean and in shallow coastal regions of the Indonesian Seas, including the Gulf of Carpentaria (Figure 2h). The impact of atmosphere ξ_{SAL_A} is clearly seen around Antarctica and southeast Asia (Figure 2g), responding to the seasonal variation in atmospheric circulation of the southern polar cell and Asian summer monsoon, respectively.

[17] In addition to annual variations, in many ocean regions a significant portion of the $\Delta\xi_{SAL}$ signal comes from subannual fluctuations. Examples include the coast around Antarctica, with $\Delta\xi_{SAL}$ signals induced by subannual changes in atmospheric pressure over Antarctica (Figure 2c), and several regions in the Southern Ocean (Figure 2d) where there is enhanced mass variability associated with ocean dynamics (Figure 1e). Notice that subannual $\Delta\xi_{SAL}$ fluctuations in the Southern Ocean exceed the typically largest annual variations. The Southern Ocean is known for the existence of several regions with large ξ_d variability at rapid time scales [e.g., *Fukumori et al.*, 1998; *Tierney et al.*, 2000; *Vinogradova et al.*, 2007] (see also Figure 1e).

[18] Interannual variations in $\Delta\xi_{SAL}$ are weaker than those at the other time scales (Figure 2i), with oceanic mass loads responsible for the largest values (Figure 2l), including those seen in several regions of the Southern Ocean and in the Gulf of Carpentaria. A caveat that should be mentioned is the relatively short period (only 7 years) used here to define the interannual variability. To evaluate the robustness of the estimated variability in Figure 2i, we computed similar interannual maps based on the 17 year long series of $\Delta\xi_{SAL}$ estimates used by *Vinogradova et al.* [2010]. The results (not shown) yielded enhanced variability in the Southern Ocean and several shallow coastal regions similar to Figure 2i, although with some differences in magnitude. More generally, the quality and realism of the interannual variability in

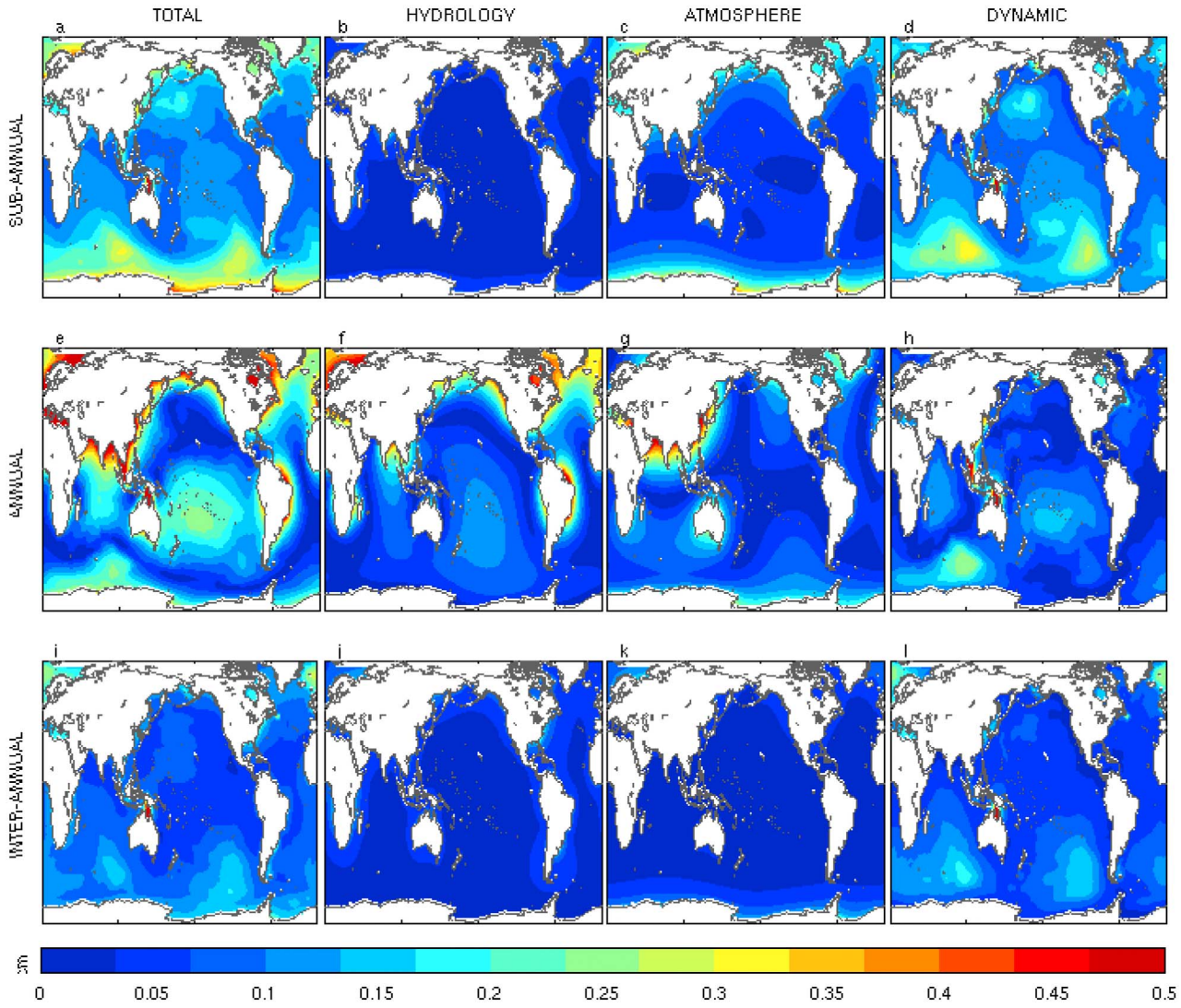

Figure 2. Variability of the SAL-induced ξ fluctuations under individual loads (ξ_{SAL_H}, ξ_{SAL_A}, ξ_{SAL_D}) and their combination ($\Delta\xi_{SAL}$) at different time scales: (a–d) subannual, (e–h) annual, and (i–l) interannual scales. Spatial mean is removed. Units are cm.

the loads evaluated here, particularly those associated with ξ_{SAL_H} and ξ_{SAL_D}, remains largely untested, and the present results should be taken as a crude order of magnitude estimate of these effects.

4. Interpreting GRACE-Derived ξ Estimates

[19] As large-scale SAL effects described in Figures 1 and 2 can affect ξ variability, we explore their role in the interpretation and understanding of ξ observations, in particular the global ξ fields derived from the GRACE mission. Such efforts gain special relevance in light of the discrepancies between GRACE-based ξ fields and those estimated from model-based efforts, including the ECCO solutions [*Ponte et al.*, 2007; *Quinn and Ponte*, 2008]. One question is whether the missing SAL physics in many of these model-based estimates can contribute to the differences found with the GRACE observations. We focus our analysis on the annual cycle to take advantage of the larger signal-to-noise ratios at this frequency. The current analysis extends that of *Vinogradova et al.* [2010] performed at only a few sites with available in situ ξ records.

[20] Figure 3 compares the ξ annual cycle from d, ξ_d, and $\xi_d + \Delta\xi_{SAL}$ fields. Spatial means have been removed from all fields. The initial ξ_d and d have similar spatial patterns, but the ξ_d amplitudes are generally much weaker (Figures 3a and 3c). Both model and data are characterized by the enhanced variability in the Southern Ocean, in the Gulf of Carpentaria, and other shallow regions where the amplitudes exceed 2 cm. A typical basin-scale phase pattern is also evident in both GRACE and ECCO, with variations in ξ in the Atlantic and Pacific basins being approximately out of phase. The annual fluctuations in Figure 3 are consistent with previous studies [e.g., *Chambers*, 2006; *Ponte et al.*, 2007; *Quinn and Ponte*, 2008; *Vinogradova et al.*, 2010]. For example, comparisons among GRACE, in situ and

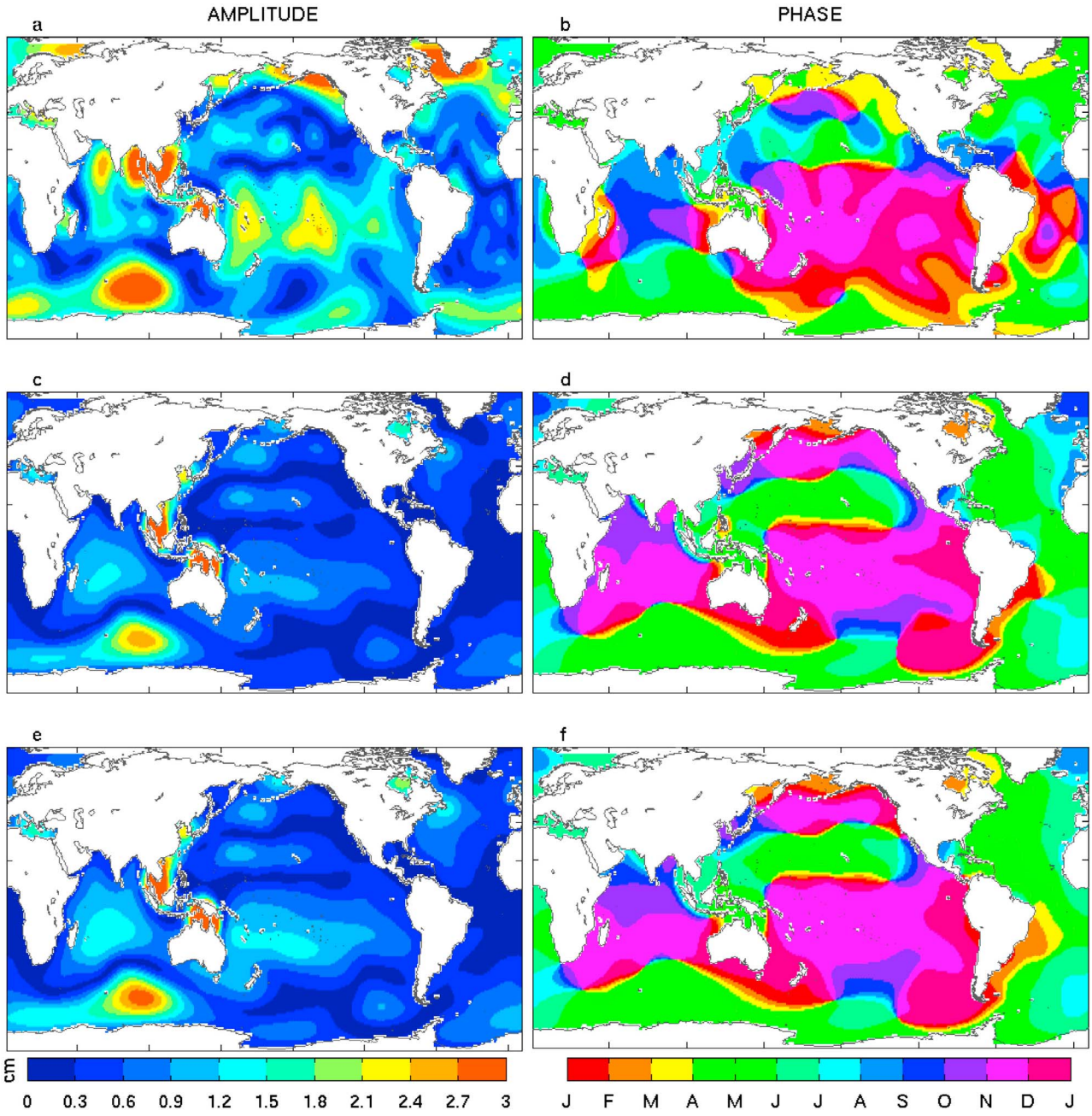

Figure 3. Annual (a, c, e) amplitude (cm) and (b, d, f) phase (months) of the GRACE data (*d*), ECCO solution (ξ_d) and ECCO + SAL series ($\xi_d + \Delta\xi_{SAL}$). The spatial mean is removed from all series. All fields are smoothed in the spherical harmonics domain with 750 km width Gaussian filter.

model-based ξ estimates show better agreement in the Southern Ocean and North Pacific [*Bingham and Hughes*, 2006; *Ponte et al.*, 2007] than in the North Atlantic [*Kanzow et al.*, 2005].

[21] Figures 3e and 3f show the annual cycle of the ECCO solution with the SAL effect included. The amplitudes in $\xi_d + \Delta\xi_{SAL}$ are generally larger than those in ξ_d, including the maxima in the Southern and Indian oceans. Amplification of the signal in the Pacific and Indian oceans is a result of $\Delta\xi_{SAL}$ being in phase with ξ_d, which is also reflected in minor phase changes of $\xi_d + \Delta\xi_{SAL}$ in these regions (cf. Figures 3f and 3d). Such behavior is expected if SAL effects act on ξ perturbations resulting from ocean internal dynamics. In other ocean regions, including Atlantic and coastal oceans, land hydrology and atmosphere SAL processes dominate, and the inclusion of $\Delta\xi_{SAL}$ can noticeably affect the annual phase in ξ (e.g., coastal oceans around Greenland and Argentina).

[22] For a quantitative measure of the impact of SAL effects based on (4), we examine the percentage gain ($\Delta\alpha > 0$) or loss ($\Delta\alpha < 0$) in the fraction of the GRACE variance that is explained when SAL effects are added to the

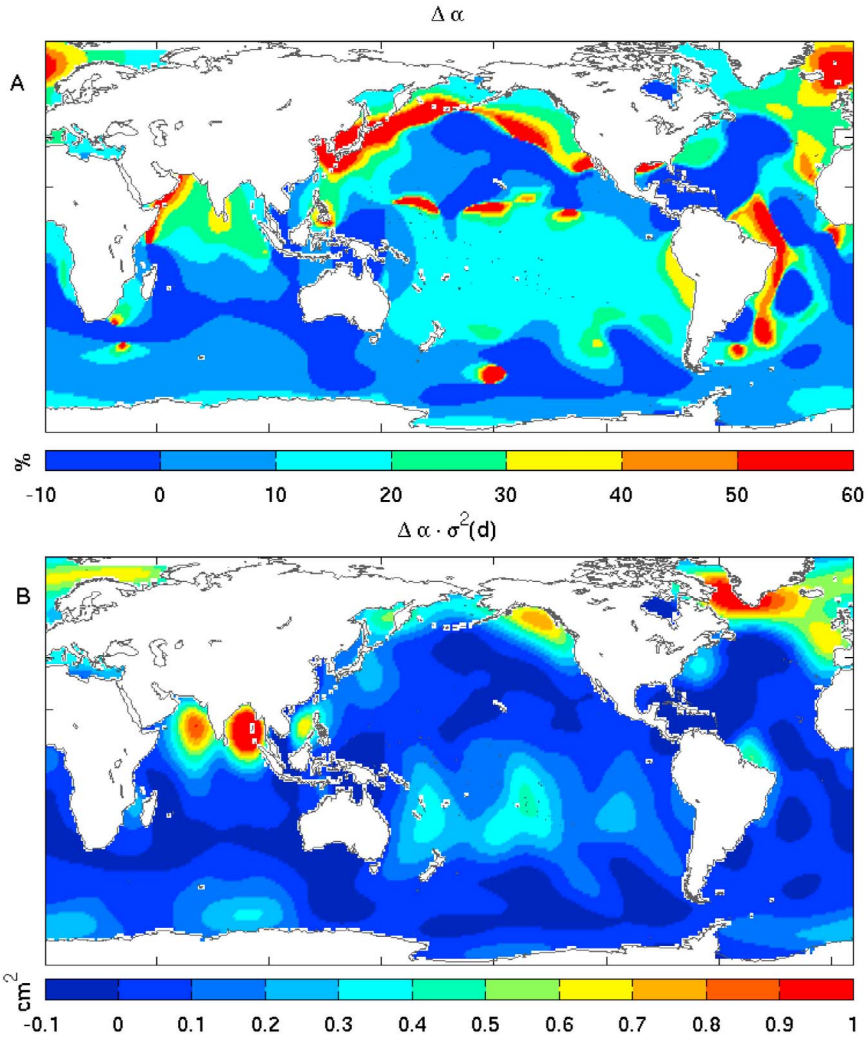

Figure 4. (a) Distribution of the increase (decrease) in percentage of annual variability, defined as the difference $\Delta\alpha$ between annual variances explained by the ECCO solution before and after SAL effects are included. Values $\Delta\alpha > 0$ indicate that the inclusion of SAL effects improves model/data agreement. (b) Distribution of the increase (decrease) in terms of data (GRACE) variance, defined as $\Delta\alpha \cdot \sigma^2(d)$.

ECCO fields (Figure 4a). On average, there is a gain in variance explained of about 16%. Typically, $\Delta\alpha > 0$ in the regions where $\Delta\xi_{SAL}$ has significant amplitude, such as regions in the South Pacific and Southern Ocean, and/or in the regions with initially poor agreement between ECCO and GRACE fields, such as in the Gulf of Alaska, Bay of Bengal and near Greenland. In terms of the absolute change (in cm^2) of the variance $\Delta\alpha \cdot \sigma^2$ (d) (Figure 4b), global average value is about +0.2 cm^2. Locally, extra variance explained by SAL effects can be >0.3 cm^2 in the South Pacific and Indian Oceans, and in the northern North Pacific and Atlantic Oceans, with additional variance explained exceeding 1 cm^2 in some regions (e.g., Bay of Bengal and around southern Greenland).

[23] To mitigate noise in the GRACE data and to examine $\Delta\xi_{SAL}$ effects at larger spatial scales, we also compare annual cycles based on averages over some regions with enhanced $\Delta\xi_{SAL}$ variability in Figure 1. The five representative regions chosen are delineated in Figure 5 and include parts of the Atlantic Ocean affected by hydrology in the Amazon River basin (30°S–10°N, 60°W–28°W), northern high latitudes (north of 57°N), parts of the Southern Ocean (south of 43°S, 50°E–117°E), Bay of Bengal (5°N–23°N, 78°E–100°E) and parts of the South Pacific (40°S–5°N, 155°E–110°W). Over each region, we compute area-weighted average series based on ξ_d, d, and $\xi_d + \Delta\xi_{SAL}$ fields and analyzed respective annual cycles shown in Figure 5.

[24] In all regions examined, the fraction of data variance explained increases appreciably when SAL effects are considered. Apart from South Pacific and Southern Ocean regions, initial agreement between GRACE and ECCO is poor, and ξ_d explains less than 10% of the observed annual variances due to large phase shifts and weak amplitudes in ξ_d. Adding $\Delta\xi_{SAL}$ affects both amplitude and phase. For example, in northern high latitudes and near the Amazon river basin, variations in ξ_d that are initially almost out of phase, become closer in phase with the data, increasing α from negative values to 21% and 46%, respectively.

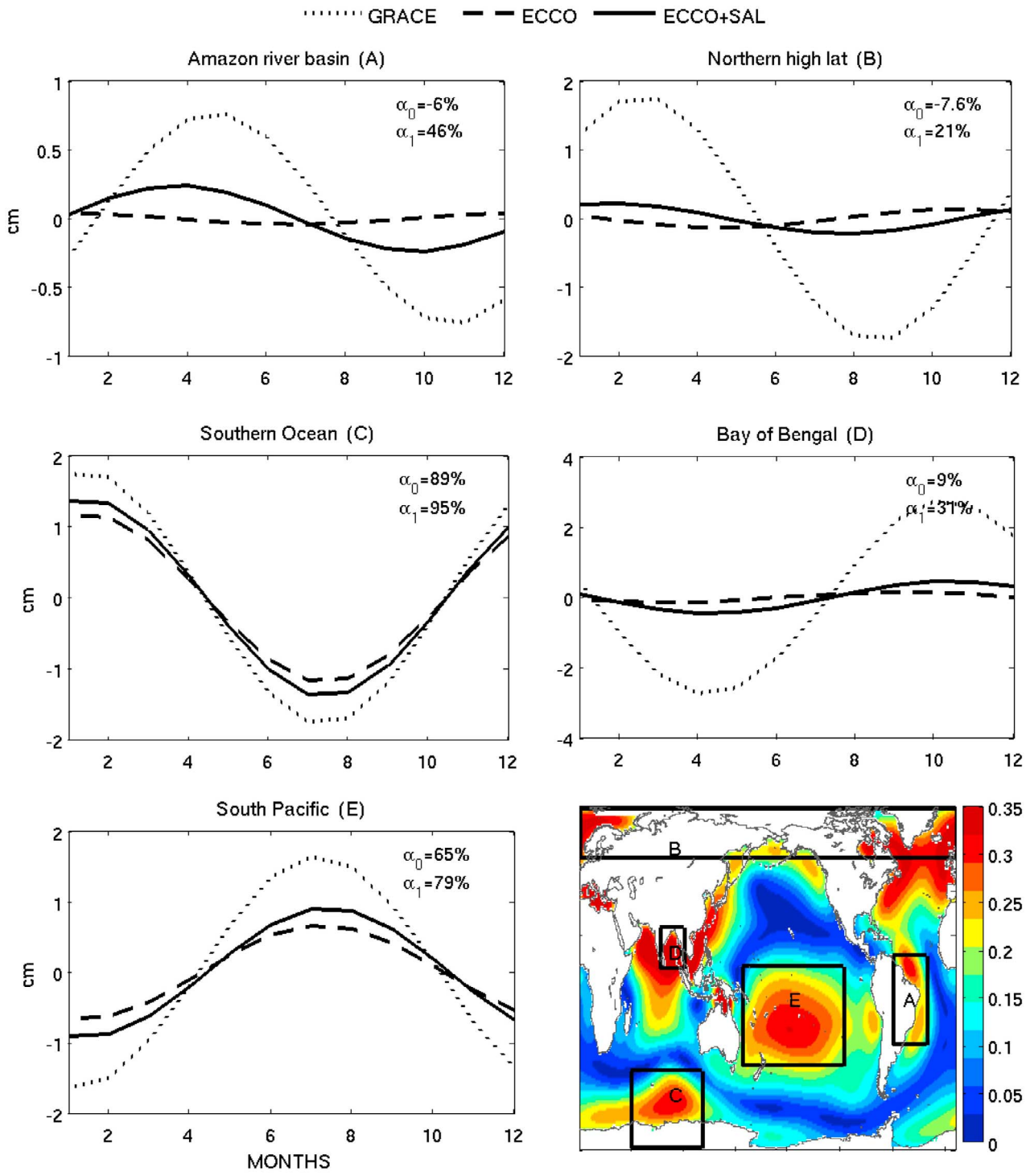

Figure 5. Annual cycle of the GRACE data, initial ECCO solution, and ECCO + SAL series averaged over selected regions. The time labeling corresponds to the middle of the month from January to December. The labeled regions (A–E) represent ocean areas with large annual amplitudes of $\Delta\xi_{SAL}$ that are shown in color on the map.

[25] In the coastal regions analyzed in Figure 5, large annual $\Delta\xi_{SAL}$ signal is driven by a strong hydrological cycle (Figure 2e). The same land hydrology signal can leak into the GRACE estimates of ξ variability, because of the inherent lack of spatial resolution of the data. Although attempts were made to remove the land signal as much as possible [*Quinn and Ponte*, 2008], further correction seems to be necessary in order to improve accuracy of the GRACE

data over the coastal oceans, particularly where $\Delta\xi_{SAL}$ (ξ_{SAL_H}) have large amplitudes, such as around Greenland and the Amazon river basin and in the Gulf of Alaska. To explore the effect of leakage, we repeated regional analysis using different land masks extending 200, 300, and 400 km away from the coast. Regardless of the land mask, adding $\Delta\xi_{SAL}$ increases the explained data variance ($\Delta\alpha > 0$) in all regions, indicating the robustness of the results discussed earlier. Also, apart from the Amazon region, the effect of land masking on α_1 (observed variance explained by $\xi_d + \Delta\xi_{SAL}$) is negligible (~1%) and does not affect our major conclusions.

[26] In addition, uncertainty in GRACE data due to leakage from continents affects mostly the amplitudes, and less the phases, of the annual cycle. The fact that the inclusion of the SAL effects modifies ξ_d phases, so as to improve the model/data agreement, is encouraging. Open ocean regions should also be less affected by land leakage errors, and this may partly explain the better agreement in amplitude and phase between ECCO and GRACE annual cycles in the South Pacific and Southern Ocean regions. Consideration of SAL effects further improves this agreement, allowing for $\xi_d + \Delta\xi_{SAL}$ to explain a substantial part of the observed variance in those regions. The examples in Figure 5 demonstrate the importance of the missing SAL component in explaining observed ξ signals, especially in regions where $\Delta\xi_{SAL}$ is significant and comparable with ξ_d signal.

5. Conclusions

[27] The exchange of water between the land, ocean and atmosphere, through the physics of SAL, can lead to significant variations in global redistribution of ocean mass and sea level, both of which are important indicators of climate change. These SAL-induced signals can cause mass fluctuations that exceed 1 cm in amplitude, which is as large as dynamic ocean mass signal in many ocean regions. The magnitude of SAL signals is not negligible at all time scales from monthly to interannual, suggesting that the SAL effects cannot be ignored in studies of ξ variability over a wide range of time scales.

[28] Each component of the ocean-land-atmosphere system results in a different SAL pattern. The nature and magnitude of $\Delta\xi_{SAL}$ is dependent on time scale and region, and all three loads can result in mass variations of considerable magnitude. Apart from several regions in the Southern Ocean, the largest variations in $\Delta\xi_{SAL}$ occur at annual time scale, mostly due to seasonal variations in water stored on land. Contribution of atmosphere and ocean dynamics is clearly seen at subannual and interannual time scales in the Southern Ocean, around Antarctica and Asia.

[29] Analysis of ξ_{SAL} changes at other frequencies would be valuable but presents certain numerical challenges. While annual (and even subannual) changes in ξ_{SAL} could be derived under the static assumption, dynamics is likely involved when calculating ξ_{SAL} effects at higher frequencies and thus inclusion of SAL physics in numerical models is required. However, explicit inclusion of these physics in ocean models has proved to be computationally expensive [e.g., *Stepanov and Hughes*, 2004; *Muller*, 2007] and, to our knowledge, has not been implemented in any available ocean circulation models. In addition to high frequencies, analysis of the long-term mass changes would also be useful for purposes of studying climate variability. To assess long-term variations in ξ_{SAL}, further improvement of hydrological models are required, including longer than seasonal contribution of snow and ice from Greenland and Antarctica and other sources to total water storage that are not currently considered in the SAL model used here.

[30] Although the different estimates of ocean mass, such as model based, satellite derived, or in situ are in good qualitative agreement, the amplitudes can be quite different. Errors in each ξ estimate can contribute to these discrepancies. Errors of model-based estimates can be attributed to many limitations in ocean models, including missing physics, inadequate forcing, inaccurate topography, coarse spatial resolution, etc. As our calculations indicate, SAL physics contributes to the difference between the model-based and observed ξ estimates in many ocean regions, with increase in annual variance of about 0.2 cm^2 (16%) on average and exceeding 1 cm^2 in some ocean regions.

[31] Improving model-based ξ estimates addresses only half of the problem and observations themselves include large uncertainties that are difficult to infer and to reduce. GRACE tends to have amplitudes larger than model-based estimates (and also larger than in situ data in some regions). Possible reasons include instrument noise as well as errors in the background models that are used in GRACE data processing. In particular, GRACE accuracy in the coastal ocean could be compromised by large land signals, which contaminate the ocean signal due to the inherent coarse resolution of GRACE measurements. Our comparison illustrates that, even with land masking applied, additional steps are required in order to correct and interpret GRACE annual amplitudes, particularly in the regions that are close to the continents with large seasonal cycle in ξ_{SAL_H}. Although concerns remain about the accuracy of the GRACE estimates in the coastal regions, the importance of SAL effects for proper interpretation of GRACE data was clearly identified.

[32] **Acknowledgments.** The work was supported by NASA grant NNX07AM77G and by the GRACE project through contract NN08CD19C to AER.

References

Bingham, R. J., and C. W. Hughes (2006), Observing seasonal bottom pressure variability in the North Pacific with GRACE, *Geophys. Res. Lett.*, *33*, L08607, doi:10.1029/2005GL025489.

Chambers, D. P. (2006), Observing seasonal steric sea level variations with GRACE and satellite altimetry, *J. Geophys. Res.*, *111*, C03010, doi:10.1029/2005JC002914.

Chambers, D. P. (2009), Calculating trends from GRACE in the presence of large changes in continental ice storage and ocean mass, *Geophys. J. Int.*, *176*, 415–419.

Chambers, D. P., M. Tamisiea, R. S. Nerem, and J. Ries (2007), Effects of ice melting on GRACE observations of ocean mass trends, *Geophys. Res. Lett.*, *34*, L05610, doi:10.1029/2006GL029171.

Clark, J. A., and J. A. Primus (1987), Sea-level changes resulting from future retreat of ice sheets: An effect of CO_2 warming of the climate, in *Sea-Level Change*, edited by M. J. Tooley and I. Shennan, pp. 256–370, Inst. of Br. Geogr., London.

Clarke, P. J., D. A. Lavallée, G. Blewitt, T. M. van Dam, and J. M. Wahr (2005), Effect of gravitational consistency and mass conservation on seasonal surface mass loading models, *Geophys. Res. Lett.*, *32*, L08306, doi:10.1029/2005GL022441.

Conrad, C., and B. H. Hager (1997), Spatial variations in the rate of sea level rise caused by present-day melting of glaciers and ice sheets, *Geophys. Res. Lett.*, *24*, 1503–1506.

Eanes, R. (2000), SLR Solutions From the University of Texas Center for Space Research, Geocenter from TOPEX SLR/DORIS, 1992–2000, http://web.archive.org/web/20071127151309/http:/sbgg.jpl.nasa.gov/datasets.html, IERS Spec. Bur. for Gravity/Geocent., Pasadena, Calif.

Farrell, W. E., and J. A. Clark (1976), On postglacial sea level, *Geophys. J. R. Astron. Soc.*, *46*, 647–667.

Fukumori, I., R. Raghunath, and L.-L. Fu (1998), Nature of global large-scale sea level variability in relation to atmospheric forcing: A modeling study, *J. Geophys. Res.*, *103*, 5493–5512, doi:10.1029/97JC02907.

Gill, A. E., and P. P. Niiler (1973), The theory of the seasonal variability in the ocean, *Deep Sea Res.*, *20*, 141–177.

Gordeev, R. G., B. A. Kagan, and E. V. Polyakov (1977), The effects of loading and self-attraction on global ocean tides: The model and the results of a numerical experiment, *J. Phys. Oceanogr.*, *7*, 161–170.

Hendershott, M. C. (1972), The effects of solid earth deformation on global ocean tides, *Geophys. J. R. Astron. Soc.*, *29*, 389–402.

Kalnay, E., et al. (1996), The NCEP/NCAR 40-year reanalysis project, *Bull. Am. Meteorol. Soc.*, *77*, 437–470.

Kanzow, T., F. Flechtner, A. Chave, R. Schmidt, P. Schwintzer, and U. Send (2005), Seasonal variation of ocean bottom pressure derived from Gravity Recovery and Climate Experiment (GRACE): Local validation and global patterns, *J. Geophys. Res.*, *110*, C09001, doi:10.1029/2004JC002772.

Losch, M., D. Menemenlis, J. M. Campin, P. Heimbach, and C. Hill (2010), On the formulation of sea-ice models. Part 1: Effects of different solver implementations and parameterizations, *Ocean Modell.*, *33*(1–2), 129–144.

Mitrovica, J., M. E. Tamisiea, J. L. Davis, and G. A. Milne (2001), Recent mass balance of polar ice sheets inferred from patterns of global sea-level change, *Nature*, *409*, 1026–1029.

Muller, M. (2007), The free oscillations of the world ocean in the period range 8 to 165 hours including the full loading effect, *Geophys. Res. Lett.*, *34*, L05606, doi:10.1029/2006GL028870.

Nakiboglu, S. M., and K. Lambeck (1991), Secular sea-level change, in *Glacial Isostasy, Sea-Level and Mantle Rheology*, edited by R. Sabadini, K. Lambeck, and E. Boschi, pp. 237–258, Kluwer Acad., Dordrecht, Netherlands.

Ponte, R. M. (1999), A preliminary model study of the large-scale seasonal cycle in bottom pressure over the global ocean, *J. Geophys. Res.*, *104*, 1289–1300.

Ponte, R. M., K. J. Quinn, C. Wunsch, and P. Heimbach (2007), A comparison of model and GRACE estimates of the large-scale seasonal cycle in ocean bottom pressure, *Geophys. Res. Lett.*, *34*, L09603, doi:10.1029/2007GL029599.

Quinn, K. J., and R. M. Ponte (2008), Estimating weights for the use of time-dependent gravity recovery and climate experiment data in constraining ocean models, *J. Geophys. Res.*, *113*, C12013, doi:10.1029/2008JC004903.

Quinn, K. J., and R. M. Ponte (2010), Uncertainty in ocean mass trends from GRACE, *Geophys. J. Int.*, *181*, 762–768, doi:10.1111/j.1365-246X.2010.04508.x.

Ray, R. D. (1998), Ocean self-attraction and loading in numerical tidal models, *Mar. Geod.*, *21*, 181–192.

Riva, R. E. M., J. L. Bamer, D. A. Lavallèe, and B. Wouters (2010), Sea-level fingerpint of continental water and ice mass change from GRACE, *Geophys. Res. Lett.*, *37*, L19605, doi:10.1029/2010GL044770.

Rodell, M., et al. (2004), The Global Land Data Assimilation System, *Bull. Am. Meteorol. Soc.*, *85*(3), 381–394.

Stepanov, V. N., and C. W. Hughes (2004), Parameterization of ocean self-attraction and loading in numerical models of ocean circulation, *J. Geophys. Res.*, *109*, C03037, doi:10.1029/2003JC002034.

Swenson, S., and J. Wahr (2006), Post-processing removal of correlated errors in GRACE data, *Geophys. Res. Lett.*, *33*, L08402, doi:10.1029/2005GL025285.

Tamisiea, M. E., E. M. Hill, R. M. Ponte, J. L. Davis, I. Velicogna, and N. T. Vinogradova (2010), Impact of self-attraction and loading on the annual cycle in sea level, *J. Geophys. Res.*, *115*, C07004, doi:10.1029/2009JC005687.

Tierney, C., J. Wahr, F. Bryan, and V. Zlotniki (2000), Short-period oceanic circulation: Implication for satellite altimetry, *Geophys. Res. Lett.*, *27*, 1255–1258.

Vinogradova, N. T., R. M. Ponte, and D. Stammer (2007), Relation between sea level and bottom pressure and the vertical dependance of oceanic variability, *Geophys. Res. Lett.*, *34*, L03608, doi:10.1029/2006GL028588.

Vinogradov, S. V., R. M. Ponte, P. Heimbach, and C. Wunsch (2008), The mean seasonal cycle in sea level estimated from a data-constrained general circulation model, *J. Geophys. Res.*, *113*, C03032, doi:10.1029/2007JC004496.

Vinogradova, N. T., R. M. Ponte, M. E. Tamisiea, J. L. Davis, and E. M. Hill (2010), Effects of self-attraction and loading on annual variations of ocean bottom pressure, *J. Geophys. Res.*, *115*, C06025, doi:10.1029/2009JC005783.

Wahr, J., M. Molenaar, and F. Bryan (1998), Time variability of the Earth's gravity field: Hydrological and ocaenic effects and their possible detection using GRACE, *J. Geophys. Res.*, *103*, 20,205–20,229.

Wouters, R., R. E. M. Riva, D. A. Lavallèe, and J. L. Bamer (2011), Seasonal variations in sea level induced by continental water mass: First results from GRACE, *Geophys. Res. Lett.*, *38*, L03303, doi:10.1029/2010GL046128.

Wunsch, C., et al. (2009), The global general circulation of the oceans estimated by the ECCO-consortium, *Oceanography*, *22*, 88–103.

J. L. Davis, Lamont-Doherty Earth Observatory, Columbia University, 61 Route 9W, Palisades, NY 10964, USA.

E. M. Hill, Earth Observatory of Singapore, Nanyang Technological University, N2-01a-15, 50 Nanyang Ave., Singapore 639798, Singapore.

R. M. Ponte, K. J. Quinn, and N. T. Vinogradova, Atmospheric and Environmental Research, Inc., 131 Hartwell Ave., Lexington, MA 02421, USA. (nadya@aer.com)

M. E. Tamisiea, National Oceanography Centre, Joseph Proudman Building, 6 Brownlow St., Liverpool L3 5DA, UK.